On the Use of Special Functions for Analyzing the Steady State Creep in Short Fiber Composites Semi-theoretically

Vahid Monfared[a]*, Saeed Daneshmand[b]

[a]Department of Mechanical Engineering, Zanjan Branch, Islamic Azad University, Zanjan, Iran
[b]Department of Mechanical Engineering, Majlesi Branch, Islamic Azad University, Isfahan, Iran

In this paper, a novel method is presented to obtain some unknowns such as displacement rate using special and well-behaved functions for short fiber composites in the steady state creep by semi-theoretical method (STM). The creep behaviors are predicted in the short fiber composites under tensile axial stress. Also, the regions under the partial debonding are predicted by the obtained results along with the reason of the partial debonding. The main purpose of this research is the use of the mathematical model instead of the time consuming and expensive experimental methods. On the other hand, the creep unknowns are simply obtained by the special functions rather than some complex theories. The use of sensor is one of the important applications of the present method in the regions with uniform behaviors. The obtained analytical results are validated by FEM results. Average difference between the analytical method and FEM results is about 10% approximately. Finally, good agreements are found between the obtained analytical and FEM results for predicting the creep behavior.

Keywords: *composite materials, creep*

1. Introduction

Recently, deformation of the short fiber composites under high stress and temperature has been studied in the scientific societies, so creep analysis become more important in various industries. Numerous researchers have investigated the steady state creep behavior using analytical and experimental methods; however, some of them have analyzed the steady state creep problems by long and time consuming methods with various considerations and assumptions.

Formerly, extensive studies have been done to determine the creep properties of the short fiber composites[1-4]. For example, viscous flow of aligned composites under tensile creep in the direction of the fibers has been studied[5]. Also, a research has been done for predicting the stress distribution in the unidirectional discontinuous fiber composites based on the shear-lag theory and the load transfer at fiber ends[6].

In the recent years, the analytical methods have been introduced for analyzing nonlinear differential and ordinary equations with purpose of obtaining suitable solutions and algorithms. In addition, some analytical and experimental attempts were carried out to analyze the creep behaviors[7-12]. For instance, a research has been carried out on the creep behavior of pre-cracked macro-synthetic fiber reinforced concrete (MSFRC) under axial tensile sustained loading[12].

In this paper, new axial and radial displacement rates are semi theoretically (analytically) presented. Also, the creep behavior of the short fiber composites is analytically predicted. The main objective of the study is to present a simple and comprehensive method to predict the steady state creep behavior of the reinforced materials. Unlike the creeping behavior of the matrix, the fibers have elastic behaviors in the

steady state creep of the short fiber composite. For example, an important discussion is briefly presented regarding the partial debonding in the creeping composites. To prevent the undesirable events, the present method can simply predict the creep rates in the second stage creep in the short fiber composites. Finally, the obtained results by the analytical and finite element (FE) methods are also compared with together in order for validating the present method for the steady state creep of the short fiber composites under axial tensile stress.

2. Material and Methods

To analyze the steady state creep problem, a cylindrical unit cell model is assumed in accordance with previous researches in order for modeling a short fiber composite[1,2,7-11]. Therefore, a unit cell of the short fiber composite is a representative for a complete composite. That is, $\dot{\varepsilon}_{composite} = (\dot{w}_{l'} / l')_{unit\ cell} = (-2\dot{u}_b / b)_{unit\ cell}$. For instance, the creep strain rate is the same for both the unit cell and complete composite (Figure 1). Thus, the unit cell model shown in Figure 1 is used for modeling the short fiber composite.

Volume fraction and aspect ratio of the fiber are respectively defined as f and $s = l / a$. In this research, the parameter "k" is defined as an important parameter in relation with the geometry of the unit cell ($k = (l' / b)/(l / a)$). An applied axial stress $\sigma_0 = \sigma_{app}$ is uniformly applied on the end faces of the unit cell (at $z = \pm l'$). A full and complete fiber-matrix interface is supposed, and the steady state creep behavior of the matrix is explained by an exponential law as the following in Equation 1.

*e-mail: vahid_monfared@alum.sharif.edu

$$\dot{\varepsilon} = X exp\left(\frac{\sigma}{\Gamma}\right) \tag{1}$$

In which, the constants of "X" and "Γ" are the creep constants obtained by the experimental methods for the creeping matrix. The deformed and undeformed shapes of the unit cell in the creeping matrix is schematically introduced in Figure 2.

Here, the related formulations are presented to determine the steady state creep behavior of the short fiber composites. The generalized constitutive equations for the small creep deformation of the matrix material in r, θ and z directions are given as the following,

$$2\sigma\dot{\varepsilon}_r = [2\sigma_r - \sigma_\theta - \sigma_z]\dot{\varepsilon} \tag{2a}$$

Figure 1. A model of the unit cell for modeling the complete short fiber composite.

Figure 2. Creeping deformed and undeformed edges in the matrix.

$$2\sigma\dot{\varepsilon}_\theta = [2\sigma_\theta - \sigma_r - \sigma_z]\dot{\varepsilon} \tag{2b}$$

$$2\sigma\dot{\varepsilon}_z = [2\sigma_z - \sigma_r - \sigma_\theta]\dot{\varepsilon} \tag{2c}$$

$$\sigma\dot{\gamma}_{rz} = 3\tau_{rz}\dot{\varepsilon} \tag{2d}$$

In which, the strain rate components are as the following,

$$\dot{\varepsilon}_r = \frac{\partial \dot{u}}{\partial r} \tag{2e}$$

$$\dot{\varepsilon}_\theta = \frac{\dot{u}}{r} \tag{2f}$$

$$\dot{\varepsilon}_z = \frac{\partial \dot{w}}{\partial z} \tag{2g}$$

$$\dot{\gamma}_{rz} = \frac{\partial \dot{w}}{\partial r} + \frac{\partial \dot{u}}{\partial z} \tag{2h}$$

In which, σ and $\dot{\varepsilon}$ are respectively equivalent stress and equivalent strain rate. The equivalent stress σ and equivalent strain rate $\dot{\varepsilon}$ are given as the following,

$$\sigma = \sqrt{\frac{(\sigma_r - \sigma_\theta)^2 + (\sigma_\theta - \sigma_z)^2 + (\sigma_z - \sigma_r)^2 + 6\tau_{rz}^2}{2}} \tag{3a}$$

$$\dot{\varepsilon} = \sqrt{\frac{2\left[(\dot{\varepsilon}_r - \dot{\varepsilon}_\theta)^2 + (\dot{\varepsilon}_\theta - \dot{\varepsilon}_z)^2 + (\dot{\varepsilon}_z - \dot{\varepsilon}_r)^2\right] + 12\dot{\varepsilon}_{rz}^2}{9}} \tag{3b}$$
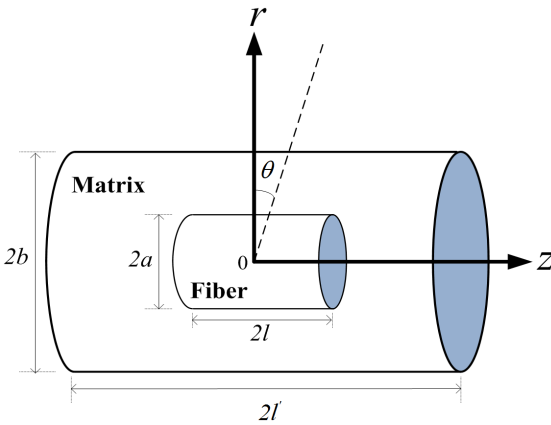
Also, incompressibility condition must be satisfied, that is

$$\dot{u}_r + \frac{\dot{u}}{r} + \dot{w}_z = 0 \tag{4}$$

At which, $\dot{u}$ and $\dot{\omega}$ are the radial and axial displacement rates.

3. Boundary Conditions

Applied boundary conditions are presented for a unit cell as a representative of a complete composite as the following,

$$\dot{u}(0,z)\big|_{l \leq z \leq l'} = 0 \tag{5a}$$

$$\dot{u}(b,z)\big|_{0 \leq z \leq l'} = \dot{u}_b \tag{5b}$$

$$\dot{w}(r,0)\big|_{a \leq r \leq b} = 0 \tag{5c}$$

$$\dot{w}(b,l)\big|_{a \leq r \leq b} = -2l\dot{u}_b / b \tag{5d}$$

$$\tau_{rz}(0,z)\big|_{0 \leq z \leq l'} = \tau_{rz}(b,z)\big|_{0 \leq z \leq l'} = \dot{\gamma}_{rz}(b,z)\big|_{0 \leq z \leq l'} = 0 \tag{5e}$$

$$\tau_{rz}(r,0)\big|_{0 \leq r \leq b} = \tau_{rz}(r,l')\big|_{0 \leq r \leq b} = 0 \tag{5f}$$

Where $\dot{u}_b$ in Equation 5b is the radial displacement rate at the outer surface of the unit cell (at $r = b$), see Figure 2.
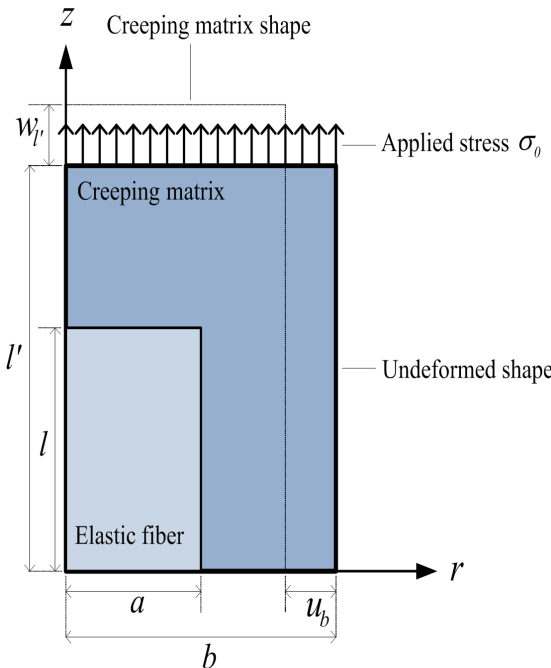
Also, the boundary conditions on the fiber/matrix interface (i.e. at $r = a$, $0 \leq z \leq l$) are as the following,

$$\dot{u}(a,z) = 0 \tag{5g}$$

$$\dot{w}(a,z) = 0 \tag{5h}$$

$$\tau_{rz}^{matrix}(a,z) = \tau_{rz}^{fiber}(a,z) = \tau_{interface} \tag{5i}$$

$$\sigma_r^{matrix}(a,z) = \sigma_r^{fiber}(a,z) = \sigma_\theta^{matrix}(a,z) = \sigma_z^{matrix}(a,z) = \sigma_{cc} \tag{5j}$$

In which, σ_{cc} is a constant value.

4. Theory and Calculation

The behavior of the steady state creep of silicon carbide whisker/6061 aluminum composite at 573 K has been predicted experimentally[2]. Here, a new mathematical and semi theoretical method (STM) is presented for analysis of the displacement rate behaviors using special functions. Also, the prediction of the creep strain rate behavior and related stresses are done analytically. Moreover, some unknowns are determined by the special functions to obtain the radial and axial displacement rates, equivalent and shear stress in steady state creep. One of the important abilities of this model is in the use of the analytical modeling instead of time consuming and expensive experimental methods.

Additionally, the present approach is very simple and straightforward for determination of the some mentioned unknowns. The results obtained by the present semi theoretical solution satisfy the equilibrium and governing, and constitutive creep equations. These analytical and semi analytical results are then validated by the finite element method (FEM). Engagingly, good agreements are found between the analytical and numerical predictions. This new approach is based on well-behaved special functions. Also, assumed displacement functions, $\dot{u}(r,z)$ and $\dot{w}(r,z)$, satisfies the B.Cs. presented in Equations 5a-d, 5g and 5h.

With considering this section, we spotlight attention on one specific power series expansion that satisfies some special function behavior. Thus far we have been using the definition of e, that is developed in most elementary calculus courses, namely, $e = \lim_{n \to \infty} (1 + (1/n))^n$. Consequently for the radial displacement rate $\dot{u}(r,z)$, we can let

$$\dot{u}(r,z) = \sum_{n=0}^{4} \lambda_n \frac{r^n}{n!}, \ for \ r \in \mathbb{C} \ (Natural \ Numbers) \tag{6}$$

Also, $\dot{w}(r,z)$ is obtained as follows,

$$\dot{w}(r,z) = -\left(\sum_{n=0}^{4} \frac{\lambda_n}{n!} r^{n-1}(1+n) \right) z \tag{7}$$

Where the coefficients of λ_n's are determined using boundary conditions presented in Equations 5a-d, 5g and 5h. In addition, shear stress behavior in the creeping matrix is analytically presented by using of Equations 1 and 2d as the following,

$$\tau_{rz} = \frac{\left[ln\left(\frac{\dot{\varepsilon}}{X} \right) \right]}{3\dot{\varepsilon}} \dot{\gamma}_{rz} \Gamma \tag{8}$$

Also, by using of Equation 1 and experimental results,[2] have

$$10^{-10.7+0.06\sigma_0} = \dot{\varepsilon} \tag{9}$$

In general, the creep strain rate in the exponential form is more precise than the polynomial and power law forms, that is,

$$\dot{\varepsilon} = X exp\left(\frac{\sigma}{\Gamma} \right) \cong X\left[1 + \frac{\sigma}{\Gamma} + \frac{\sigma^2}{2!\Gamma^2} + ... \right] = \left[X + \frac{X\sigma}{\Gamma} + \frac{X\sigma^2}{2!\Gamma^2} + ... \right] = \sum_{i=0}^{n} a_i x^i \tag{10}$$

Therefore, polynomial and power law functions are only a small part of the exponential function expansion. So, we can use the polynomial and power law functions instead of exponential law generally. Now, the displacement rate $\dot{u}_b$ is determined by exponential form of the creeping matrix approximately. Furthermore, displacement rate is obtained without using some theories in the steady state creep in the short fiber composites. Effective factor or coefficient is presented to obtain the creep displacement rate. With employing Equations 1 and 9 have,

$$\dot{u}_b = -0.5 \left[b(10^{-10.7+0.06\sigma_0}) \right] \times \xi \tag{11}$$

$$\dot{u}_b = X exp\left(\frac{\sigma_0}{\Gamma} \right) \times \xi = \frac{b\dot{\varepsilon}_{composite}}{-2} \tag{12}$$

Where, ξ is an effective factor, that is,

$$\xi \propto \xi(\sigma_0, f, k, s) \tag{13}$$

Then, ξ is obtain by above information, yields

$$\xi \cong exp(-\sigma_0 \times \Pi) \tag{14}$$

So,

$$\dot{u}_b = X exp\left(\frac{\sigma_0}{\Gamma} \right) \times exp(-\sigma_0 \times \Pi) \tag{15}$$

By using of the geometrical relations have,

$$\dot{\varepsilon}_{composite} = -\frac{2}{b} \left[X exp\left(\frac{\sigma_0}{\Gamma} \right) \times exp(-\sigma_0 \times \Pi) \right] \tag{16}$$

In which, the unknown parameter of Π is semi theoretically obtained by analytical, FEM and available experimental results as the following,

$$\Pi = ln(X) + 4\Gamma - \left(\frac{l'a}{lb} \right) - bf \tag{17}$$

So, the simplified form of the radial displacement rate at the outer surface of the unit cell $\dot{u}_b$ (at $r = b$) is in the following form,

$$\dot{u}_b = X\left[exp\left(\frac{\sigma_0}{\Gamma} - \sigma_0 ln \, X - 4\Gamma\sigma_0 + \frac{l'a}{lb}\sigma_0 + bf\sigma_0 \right) \right] \tag{18}$$

Approximate Maclaurin expansion of Equation 18 for $n = 4$ along with the weighted functions of p_1, p_2, p_3, p_4, and p_5, in the exponential form is as the following function,

$$\frac{\dot{u}_b}{X} = lp_1 + \left(\frac{\sigma_0}{\Gamma} - \sigma_0 ln\,X - 4\Gamma\sigma_0 + \frac{l'a}{lb}\sigma_0 + bf\sigma_0\right)p_2 +$$

$$\frac{\left(\frac{\sigma_0}{\Gamma} - \sigma_0 ln\,X - 4\Gamma\sigma_0 + \frac{l'a}{lb}\sigma_0 + bf\sigma_0\right)^2}{2!}p_3 +$$

$$\frac{\left(\frac{\sigma_0}{\Gamma} - \sigma_0 ln\,X - 4\Gamma\sigma_0 + \frac{l'a}{lb}\sigma_0 + bf\sigma_0\right)^3}{3!}p_4 + \qquad (19)$$

$$\frac{\left(\frac{\sigma_0}{\Gamma} - \sigma_0 ln\,X - 4\Gamma\sigma_0 + \frac{l'a}{lb}\sigma_0 + bf\sigma_0\right)^4}{4!}p_5$$

The coefficients of p_1, p_2, p_3, p_4 and p_5 are obtained by semi theoretical, analytical, FEM, and experimental results using MATLAB software code (programming) and neural network method. After obtaining the weighted coefficients of p_1, p_2, p_3, p_4 and p_5 by the mentioned methods, and simplification of the polynomial function to the power function, the following formulation is presented simply,

$$\dot{u}_b = 3 \times 10^{-43} \sigma^{18.685} \qquad (20)$$

The similar results for the parameter of Π are obtained using the other semi theoretical approaches. The behavior of the parameter of Π depends on the variations of the geometrical factors and material properties. This parameter may be obtained by determining displacement rates and available experimental results with consideration of the applied boundary conditions (Equations 5a-j).

5. Results and Discussions

To verify the present method, the SiC_{fiber}/Al_{matrix} composite is chosen as a case study and the obtained results are compared with the FEM results. For the composite used here, SiC_{fiber}/Al_{matrix}, the volume fraction of fibers f is 0.15 and the fibers have an aspect ratio (s) of 7.4 and $k = 0.76$, which are in accordance with the suggestions made in the reference.[2] For comparison purpose, the finite element numerical calculations of creep behavior of this short fiber composite are also performed using the finite element commercial code of ANSYS. The axisymmetry method with non-linear quadratic element is used for finite element method (FEM). This element is a higher order eight-node element and has creep modeling ability (Note that, $X = exp(-24.7)$, $\Gamma = 6.47$)). The axisymmetry approach with nonlinear quadratic element is utilized for FEM analysis. Contour nodal solution data for analyzing the strain rate in r-direction, shear stress, and strain rate behaviors are presented by the analytical present method and FEM (Figures 3-5).

For instance, a simple and general representation of the FE model with boundary conditions and coupling conditions under tensile axial loading are shown in Figures 3a, b.

The marked region in Figure 3c shows the high possibility for occurring the partial debonding because of the high total mechanical strain in the r-direction in the mentioned

region. So, this high possibility for occurring the partial debonding should be considered in the composite design under high stress and temperature. In addition, the comparison between the obtained analytical work and finite element method (FEM) results are shown in Figures 4, 6, 7 and 8.

It is interesting that the gradients of the shear stress values at the region located at $0.75l \leq z \leq l$, $r = a + \delta$ are very small. However, this gradient is high at the region located at $0 \leq z \leq 0,25l$, $r = a + \delta$. These changes in the gradients are because of the nature of the tensile steady state creep phenomenon in the short fiber composites.

In which, δ is small enough and also positive. Moreover, the average obtained results are presented to determine the total strain rate behavior in r-direction at $r = b$, $0 < z < l$ in the creeping matrix with assumption of $a=1$ (Figure 5).

In Figure 5, the behavior of the average total mechanical strain rate is steady and uniform (constant value of 4.2×10^{-3} at $1.5 \leq z \leq 6$). The behavior of the mentioned region at $1.5 \leq z \leq 6$ is steady and favorable for composite design. Also, the region is safe because, the sudden and unexpected behavior such as surprising creep rupture is not seen in the region, and the behavior is smooth and uniform. As an important application, using sensors for controlling and tracking the creep deformations in the mentioned region can be desired and be safe due to uniform behavior of the creeping matrix.

Figure 6 shows an important relation between the shear stress and shear strain rate at $r = a + \delta$ in the creeping matrix. The following formulation defines the mentioned relation between the shear stress and shear strain rate at $r = a + \delta$ in the creeping matrix in the polynomial form as below,

$$\dot{\varepsilon}_{rz} = 2 \times 10^{-14} \tau_{rz}^6 - 2 \times 10^{-12} \tau_{rz}^5 +$$
$$5 \times 10^{-11} \tau_{rz}^4 - 8 \times 10^{-10} \tau_{rz}^3 + \qquad (21)$$
$$5 \times 10^{-9} \tau_{rz}^2 - 10^{-8} \tau_{rz} + 10^{-9}$$

In addition, shear strain rate behavior with respect to the normalized axial position is shown in Figures 7 and 8.

The obtained results show that shear strain rate behavior is smooth and soft at $r = a + \delta$ and $r = a - \delta$ in the creeping matrix. Therefore, these smooth and soft gradients and slopes in the curves are because of the nature of the second stage creep of the matrix in the short fiber composites.

Therefore, in order for preventing the undesirable events, we can control and predict the related creep rate behaviors in the steady state creep of the short fiber composite in accordance with the obtained results by present method.

Table 1 shows that the obtained results by the present semi-theoretical approach and FEM are similar to the experimental data.[2] So, it is concluded that the present semi-theoretical method can be a beneficial, simple, and efficient approach for obtaining the creep unknowns such as the radial displacement rate at the outer surface ($\dot{u}_b$), and also predicting the creep behavior in the short fiber composites.
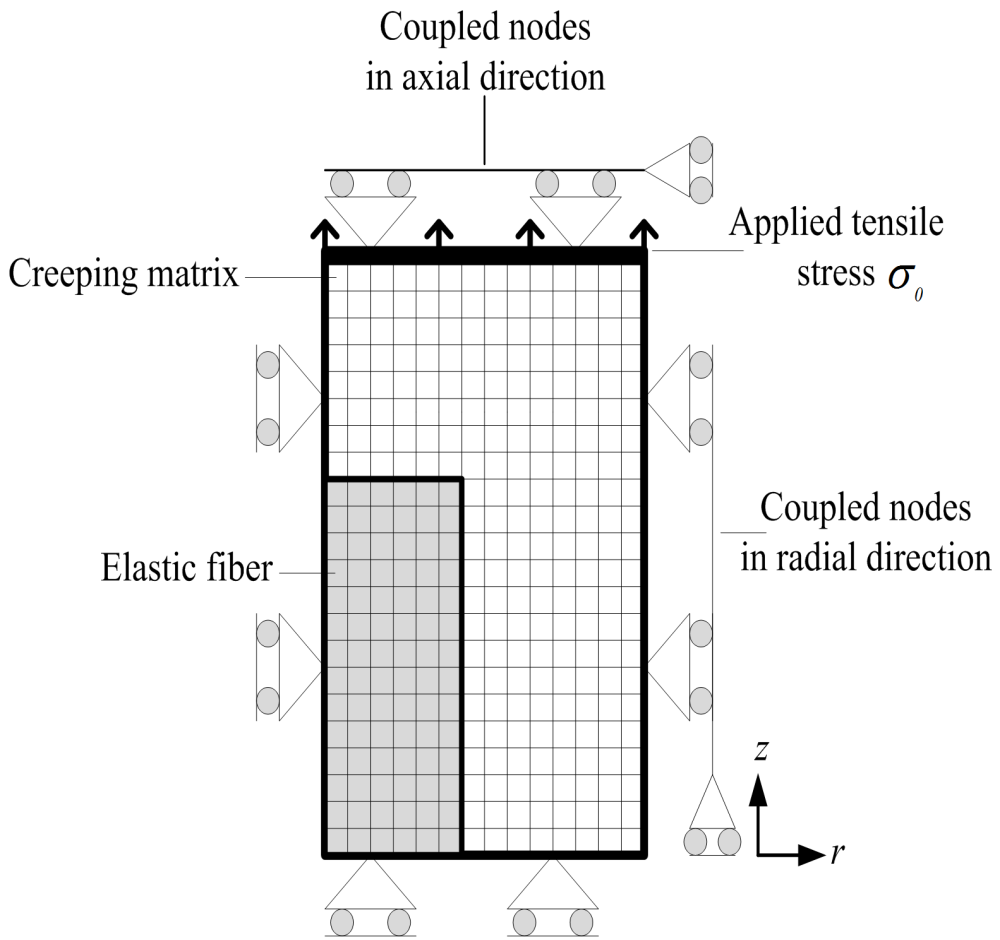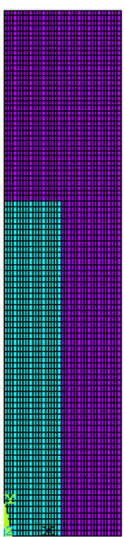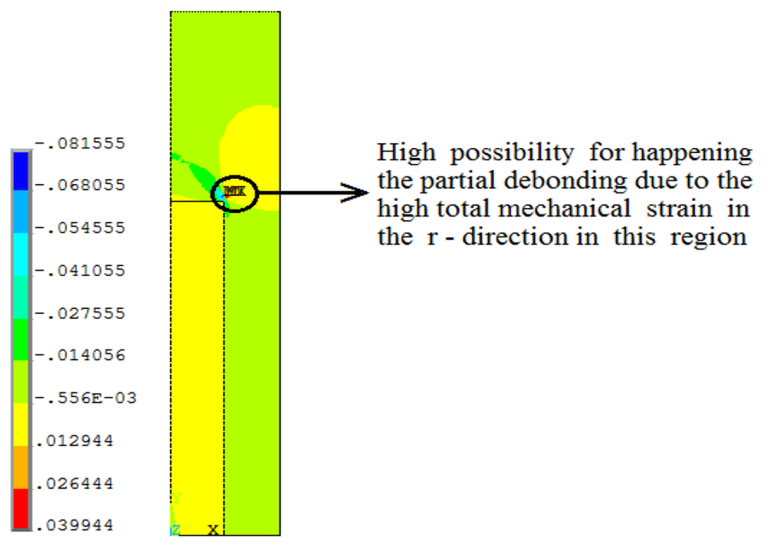
Figure 3. (a) Axisymmetric model of the finite element in unit cell (b) FEM meshing (c) Contour nodal solution data to analyze the r-component of total mechanical strain [x = r (radial), y = z (axial), z = θ circumferential)].
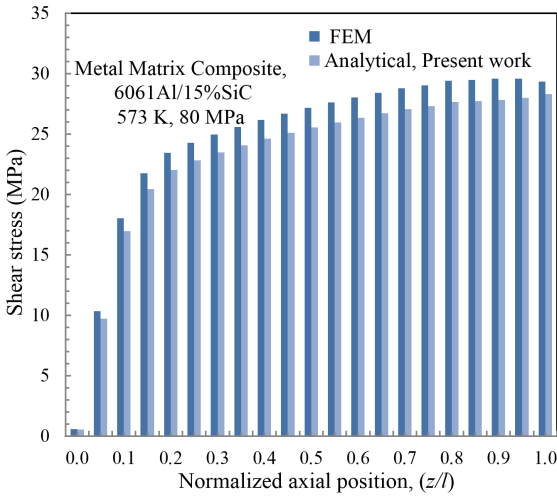
Figure 4. Behavior of the shear stress at $r = a + \delta$ by FEM and STM (Analytical, present work).
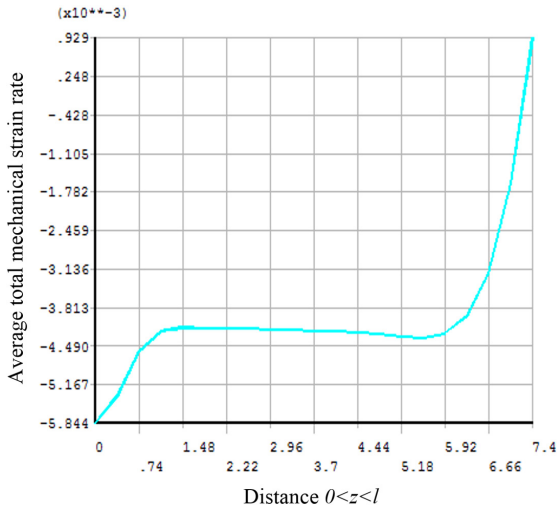

Figure 5. The average obtained results for achieving total strain rate behavior in r-direction at $r = b$, $0 < z < l$ in the creeping matrix with assumption of $a=1$.
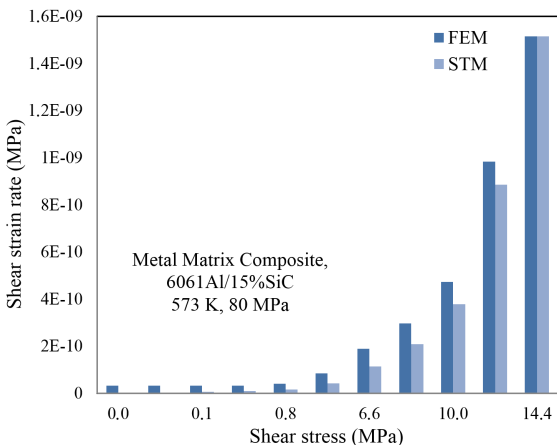

Figure 6. The relation between shear strain rate and shear stress at $r = a + \delta$.
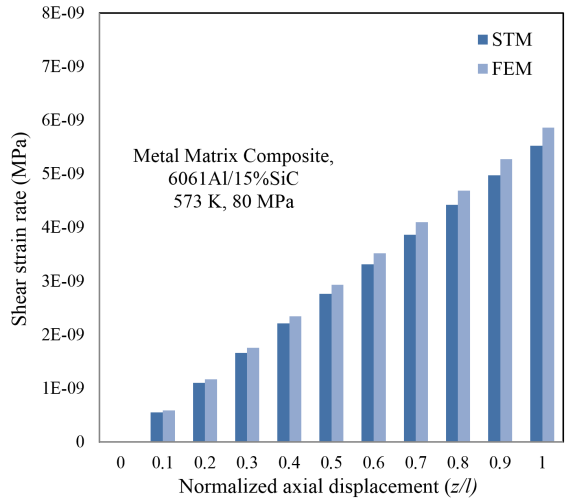

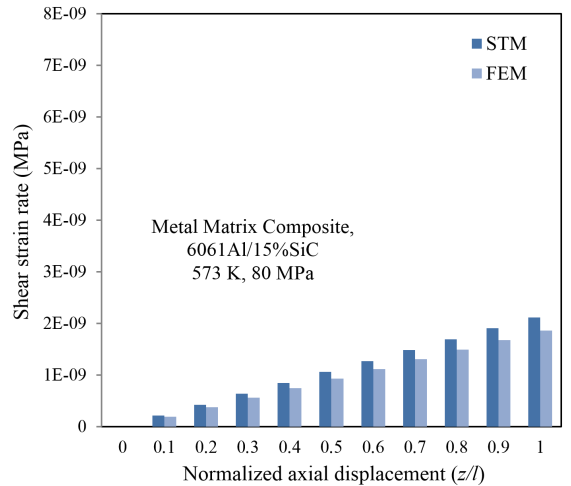**Figure 7.** Shear strain rate behavior at $r = a + \delta$.

Figure 8. Shear strain rate behavior at $r = a - \delta$.

Table 1. Comparison between the obtained results and experimental data[2] for obtaining the radial displacement rate at the outer surface ($\dot{u}_b$).

	Composite 6061Al/15%SiC		
Applied stress (MPa)	Methods		
	STM (Present work)	Experimental[2]	FEM (Present work)
70	8.96×10^{-9}	7.58×10^{-9}	7.981×10^{-9}
86	4.19×10^{-7}	3.70×10^{-7}	3.736×10^{-7}
90	9.82×10^{-7}	6.59×10^{-7}	8.742×10^{-7}
95	2.69×10^{-6}	2.10×10^{-6}	2.411×10^{-6}
100	7.03×10^{-6}	6.59×10^{-6}	6.255×10^{-6}

6. Conclusions

According to the research, the following results can be concluded,

- The obtained results by the analytical and semi-theoretical methods are similar to the results obtained by FEM. The method is simpler than the other available methods for creep analyzing.

- The radial and axial displacement rates are determined using the well-behaved special functions by STM. Also, relation between the shear stress and shear strain rate was obtained at $r = a + \delta$ in the creeping matrix in the polynomial form by present method along with effective factor and coefficient.

- One of the advantages of the mentioned method is using of the mathematical modeling instead of time consuming and costly experimental methods, and complex methods.

- At the end of the fiber, the possibility of occurrence of the partial debonding is high because of the high total mechanical strain in the r-direction in the mentioned region.

- Use of the sensors in the regions with uniform and steady strain rate is one of the important applications of the present method.

- Finally, in order to prevent the undesirable events, the present method can simply predict the creep rate behaviors in the steady state creep of the short fiber composites.

References

1. Cox HL. The elasticity and strength of paper and other fibrous materials. *British Journal of Applied Physics*. 1952; 3(3):72-79. http://dx.doi.org/10.1088/0508-3443/3/3/302.

2. Morimoto T, Yamaoka T, Lilholt H and Taya M. Second stage creep of silicon carbide whisker/6061 aluminum composite at 573 K. *Journal of Engineering Materials and Technology*. 1988; 110(2):70-76. http://dx.doi.org/10.1115/1.3226032.

3. Lee YS, Batt TJ and Liaw PK. Stress analysis of a composite material with short elastic fibre in power law creep matrix. *International Journal of Mechanical Sciences*. 1990; 32(10):801-815. http://dx.doi.org/10.1016/0020-7403(90)90160-K.

4. Khadraoui F. Creep and shrinkage behavior of CFRP-reinforced mortar. *Construction & Building Materials*. 2012; 28(1):282-286. http://dx.doi.org/10.1016/j.conbuildmat.2011.07.048.

5. McLean D. Viscous flow of aligned composites. *Journal of Materials Science*. 1972; 7(1):98-104. http://dx.doi.org/10.1007/BF00549556.

6. Fukuda H and Chou TW. An advanced shear-lag model applicable to discontinuous fiber composites. *Journal of Composite Materials*. 1981; 15(1):79-91. http://dx.doi.org/10.1177/002199838101500107.

7. Tapkın S, Çevik A, Uşara U and Gülşan E. Rutting prediction of asphalt mixtures modified by polypropylene fibers via repeated creep testing by utilising genetic programming. *Materials Research*. 2013; 16(2):277-292.

8. Reis JF So. and Bueno LO. Hot tensile and creep rupture data extrapolation on 2.25Cr-1Mo steel using the CDM penny-kachanov methodology. *Materials Research*. 2014; 17(2):518-526. http://dx.doi.org/10.1590/S1516-14392014005000007.

9. Costa PR Jr., Moura C No. and Wade DA. Evaluation of a 7050-TAF aluminum alloy submitted to creep age forming. *Materials Research*. 2014; 17(3):603-611. http://dx.doi.org/10.1590/S1516-14392014005000051.

10. Monfared V and Mondali M. Semi-analytically presenting the creep strain rate and quasi shear-lag model as well as finite element method prediction of creep debonding in short fiber composites. *Materials & Design*. 2014; 54:368-374. http://dx.doi.org/10.1016/j.matdes.2013.08.040.

11. Monfared V, Daneshmand S and Monfared AH. Effects of atomic number and atomic weight on inelastic time dependent deformations. *Kovove Materialy-Metallic Materials*. 2015; 53(2):85-89.

12. Babafemi AJ and Boshoff WP. Tensile creep of macro-synthetic fibre reinforced concrete (MSFRC) under uni-axial tensile loading. *Cement and Concrete Composites*. 2015; 55:62-69. http://dx.doi.org/10.1016/j.cemconcomp.2014.08.002.